ResearchGate

See discussions, stats, and author profiles for this publication at: https://www.researchgate.net/publication/49648965

Tuning the Morphology of Cellulose Acetate Gels by Manipulating the Mechanism of Phase Separation

ARTICLE *in* BIOMACROMOLECULES · JANUARY 2011

Impact Factor: 5.75 · DOI: 10.1021/bm100917j · Source: PubMed

CITATIONS
4

READS
12

2 AUTHORS, INCLUDING:

Reza Korehei
University of British Columbia - Vancouver
10 PUBLICATIONS **33** CITATIONS

SEE PROFILE

Available from: Reza Korehei
Retrieved on: 31 January 2016

Tuning the Morphology of Cellulose Acetate Gels by Manipulating the Mechanism of Phase Separation

John F. Kadla* and Reza Korehei

Advanced Biomaterials Chemistry, Faculty of Forestry, University of British Columbia, Vancouver, British Columbia V6T 1Z4 Canada

Received August 6, 2010; Revised Manuscript Received November 13, 2010

The effect of dihydric alcohol (nonsolvent) addition on the rheological and microstructural behavior of cellulose acetate (CA) in a ternary CA, *N*,*N*-dimethylacetamide (DMA), nonsolvent system was investigated. Increasing the dihydric alcohol concentration led to enhanced steady shear viscosity and dynamic viscoelastic properties that were dependent on CA concentration. Changing the dihydric alcohol from 1,2-ethanediol to 1,4-butanediol and 1,6-hexanediol increased the moduli and decreased the concentration of nonsolvent at which the sol−gel transition occurred. At 10 wt % CA concentration the modulus and gel morphology of the 1,2-ethanediol and 1,4-butanediol systems were quite similar and distinctly different from that of 1,6-hexanediol. In the former, the gel morphologies were more heterogeneous, evident of more extensive coarsening, and likely obtained via nucleation and growth and spinoidal decomposition of off-critical mixtures. The latter exhibited more uniform dense network morphology, indicative of a spinoidal decomposition of near-critical mixtures. The gels were fractal in nature and exhibited different fractal dimensions in-line with the observed differences in microstructure; $D \sim 1.87 \pm 0.02$ (1,2-ethanediol and 1,4-butanediol) and $D \sim 1.97 \pm 0.02$ (1,6-hexanediol). However, at 15 wt % CA content, the gels exhibited more similar viscoelastic behavior and gel microstructures; $D \sim 1.97 \pm 0.02$ for all three dihydric alcohol systems.

Introduction

In filtration, membrane, and encapsulation applications sophisticated network structures are required. This is typically achieved through aggregation-induced phase separation (Khalil 1973; Pilon et al. 1971), which can be induced by solvent evaporation, changes in temperature, or the addition of a nonsolvent (Vogrin et al. 2002). In non-solvent-induced phase separation, the concentration of polymer, solvent, and nonsolvent are critical (Kunst and Sourirajan 1970; Matsuyama et al. 2000). Depending on the system, phase separation can lead to physical gel formation; a result of polymer aggregation and the formation of large macromolecular associates and clusters (Reuvers et al. 1986; Hao and Wang 2001). The viscoelastic behavior of the gel/solid network is highly dependent on the chemical/physical structure of the polymer and the functional groups available on the solvent/nonsolvent. Polymer−polymer, polymer−solvent, and solvent−nonsolvent interactions all play a role in network formation. For various polymeric systems, dipole moments and donor−acceptor properties of each component, as well as the strength of hydrogen bonding, have been used to explain the process of gel formation.[1−3]

Recently we reported the effect of hydrophilic and hydrophobic interactions on the rheological behavior and microstructure of a ternary cellulose acetate system.[4] The sol−gel transition and resulting gel morphology was dependent on nonsolvent structure. Increasing the available hydrogen bonding groups within the nonsolvent led to higher modulus (stronger gels) and a sol−gel transition at lower nonsolvent concentration. Similarly, increasing the alkyl chain length (hydrophobicity) of the nonsolvent also enhanced the viscoelastic properties, however, hydrogen bonding, specifically the ability to hydrogen-bond donate, was critical for gel formation. The phase-separated gel morphologies were quite distinct, with increasing hydrophilic interactions leading to more uniform and dense networks, consistent with a spinoidal decomposition mechanism of near critical mixtures; whereas, on the other hand, the hydrophobic nonsolvents produced more heterogeneous phase-separated gel networks, likely via nucleation and growth and spinoidal decomposition of off-critical mixtures: the extent of microstructure coarsening increasing with increasing hydrophobicity.

To further explore the impact of nonsolvent structure on cellulose acetate gel formation and exploit the differences in phase-separation mechanism, a series of dihydric alcohol nonsolvents were investigated in an attempt to control and tune gel morphology. Using steady shear and dynamic rheology and confocal microscopy, we assess the impact of a series of dihydric alcohols with increasing alkyl chain length (1,2-ethanediol, 1,4-butanediol, and 1,6-hexanediol) on the resulting viscoelastic properties and gel microstructure.

Experimental Section

Materials. Cellulose acetate (CA, M_n ca. 30000 g/mol, degree of acetylation (DA) = 2.45 (39.7 wt % acetyl content)), HPLC grade *N*,*N*-dimethylacetamide (DMA), 1,2-ethanediol (1,2-ED), 1,4-butanediol (1,4-BD), and 1,6-hexanediol (1,6-HD) were purchased from Sigma-Aldrich and used as received.

Sample Preparation. All samples were prepared from a bulk 28 wt % CA in DMA solution. To ensure a homogeneous solution and facilitate adequate dissolution of the CA in the DMA, the mixture was heated at 100 °C for 10 min under a blanket of nitrogen and allowed to cool to room temperature prior to use. The specific CA/DMA/nonsolvent concentrations used in this study were obtained by adding appropriate amounts of nonsolvent and DMA to the 28 wt % CA/DMA stock solution. The samples were mechanically mixed, blanketed with nitrogen, and heated to 100 °C for 10 min to ensure complete miscibility

* To whom correspondence should be addressed. E-mail: john.kadla@ubc.ca.

10.1021/bm100917j © 2011 American Chemical Society
Published on Web 12/01/2010

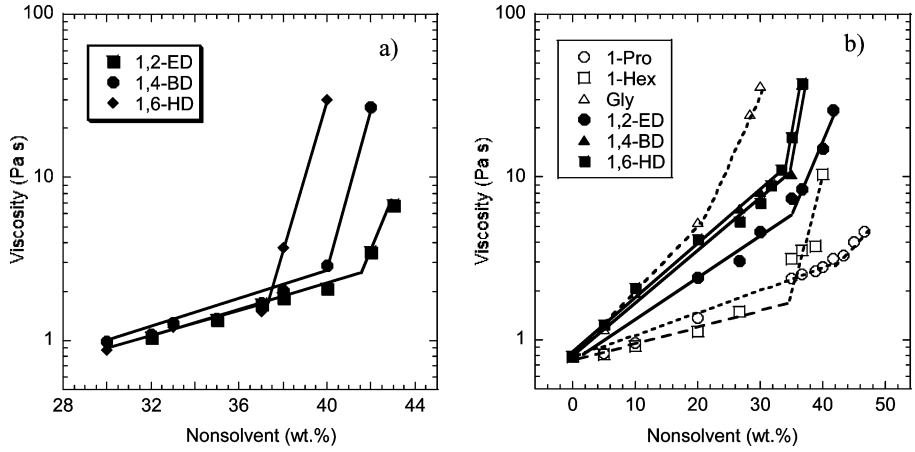

Figure 1. Effect of dihydric alcohol content on the viscosity enhancement of the CA/DMA/nonsolvent solutions (data represents zero-shear viscosity) at (a) 10 wt % and (b) 15 wt % CA content, respectively: 1,2-ethanediol (1.2-ED); 1,4-butanediol (1,4-BD); 1,6-hexanediol (1,6-HD); also included are 1-propanol (1-Pro), 1-hexanol (1-Hex), and glycerol (Gly).[4]

and left at ~25 °C for exactly 1 week in a desiccator prior to analysis. All solutions and dilutions were prepared on a weight basis.

Rheological Characterization. All rheological experiments were performed at 25 °C using a TA Instruments AR 2000 Rheometer with either a 60 mm diameter aluminum, 2° cone angle, or a stainless steel parallel plate (20 mm diameter) geometry. For gel samples, a variable gap (1000−2000 μm) was used based on a constant applied force (<0.2 N cm^{-2}). In the dynamic experiments the samples were subjected to a sinusoidal deformation as a function of increasing strain amplitude or frequency of oscillation, and the corresponding elastic (G') and viscous (G'') moduli were measured. Dynamic stress sweep experiments were performed to determine the linear viscoelastic (LVE) regime prior to the frequency sweep experiments.

Fourier Transform Infrared (FTIR) Spectroscopy. FTIR spectra were measured on a Perkin-Elmer 16PG FTIR spectrometer. A total of 16 scans were collected at a resolution of 4 cm^{-1} over the range of 400 to 4000 cm^{-1}. FTIR spectra were collected using 10 mg samples positioned between ZnSe salt plates. Care was taken not to disrupt sample microstructure during the transfer and positioning between the plates, which were set at a ~3−5 mm gap.

Confocal Laser Scanning Microscopy (CLSM). A confocal laser scanning system (Chameleon, compact ultra fast Ti) connected to an inverted microscope (Zeiss Axiovert) was used to analyze the gels. Calcofluor white (0.01 wt %, based on CA) was used to tag the CA for CLSM.[1] All samples were prepared as per the rheology experiments, with the exception that calcofluor white (0.01 wt %) was added at the time of CA dissolution. The samples were then heated and a few drops of the hot bubble-free solution were placed onto a single concavity microscopy slide and covered with a 0.5 mm thick coverslip. The samples were then conditioned for 1 week in a desiccator at ambient temperature. Optical sectioning was performed as a function of the depth along the z-axis. The IR laser excitation source was set to 705 nm with two channel spectra detection (Ch1 filter: 544−704 nm, Ch2 filter: 435−485 nm). Scans were collected as stack images with a stack size of X, 142.86 μm; Y, 142.86 μm; and Z, 27.87 μm.

Data Analysis. All rheological analyses were within an error of less than 10%. The error was determined by running multiple replicates per sample (minimum of four replicates per sample). In the CLSM experiments, image analysis was done using Adobe Photoshop 7.0 (Adobe Systems Inc.). Fractal dimensions were determined from CLSM from five layers through the sample thickness and analyzed by Image J software (NIST) using the fractal box count method. Average fractal dimension and standard deviation were obtained.

Results and Discussion

The addition of dihydric alcohols (nonsolvent) to CA/DMA solutions leads to an enhancement in viscosity with increasing nonsolvent addition. In all samples, the typical large Newtonian plateau was observed at low nonsolvent content followed by shear thinning at high shear rates (Figure S1 of the Supporting Information). Increasing the nonsolvent content increased the viscosity to higher values and shifted the onset of shear thinning to lower shear rates.[1,4,5] Figure 1 illustrates the change in zero-shear viscosity with increasing dihydric alcohol content at 10 and 15 wt % cellulose acetate concentration.

The ternary systems display a progressive increase in shear viscosity with increasing nonsolvent followed by a dramatic change in slope of the viscosity versus nonsolvent content plot at higher dihydric alcohol contents.[4] At 10 wt % CA concentration, the initial slope was the same for the three nonsolvents, but the change in slope occurred at lower nonsolvent content with increasing alkyl chain length of the dihydric alcohol, that is, 1,6-hexanediol (~37 wt.%) < 1,4-butanediol (~40 wt %) < 1,2-ethanediol (~42 wt %). By contrast, at 15 wt % CA, the initial slopes of the 1,6-hexanediol and 1,4-butanediol systems where approximately the same, but greater than that of the 1,2-ethanediol system. However, the change in slope occurred at approximately the same nonsolvent content, ~35 wt %, regardless of the nonsolvent.

Comparison between the results for the 15 wt % CA systems (Figure 1b) revealed distinct similarities with previous results obtained using various monohydric and polyhydroxyl alcohols.[4] The initial slopes of the dihydric alcohol viscosity versus nonsolvent content plots were significantly higher than those of the previously studied monohydric alcohols (1-propanol and 1-hexanol, included in Figure 1b) and in-line with that of glycerol, but only showing a slight dependence on alkyl chain length: 1,6-hexanediol ~ 1,4-butanediol > 1,2-ethanediol. This seems to indicate that intermolecular interactions such as hydrogen bonding are playing a role in increasing the shear viscosity of the systems.[4] However, at higher nonsolvent contents, the 1,6-hexanediol and 1,4-butanediol systems increase in viscosity much more rapidly with nonsolvent content than the 1,2-ethanediol system. At these higher nonsolvent contents the behavior of the 1,6-hexanediol and 1,4-butanediol systems are more comparable to that of 1-hexanol, while the 1,2-ethanediol systems more closely resembles that of glycerol.

Previously we found that increasing the propensity of the nonsolvent to participate in intermolecular interactions contributed to microstructure development and viscosity enhancement.[1,4,5] In dilute solutions hydrophilic interactions such as hydrogen bonding had a greater effect on viscosity than hydrophobic

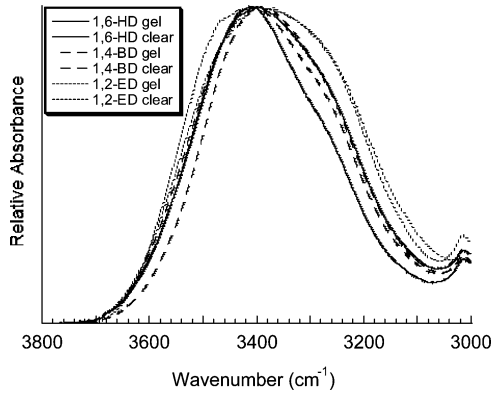

Figure 2. FTIR spectra of the hydroxyl stretching region of CA/DMA/nonsolvent solutions at 15 wt % CA concentration and 26.6 wt % (clear) and 40.0 wt % (gel) nonsolvent contents: 1,2-ethanediol (1,2-ED); 1,4-butanediol (1,4-BD); 1,6-hexanediol (1,6-HD).

interactions. Increasing the number of hydroxyl groups on the nonsolvent increased hydrogen bonding between constituents, and lead to an increase in viscosity. However, at higher nonsolvent contents, viscosity enhancement occurred faster in the hydrophobic nonsolvent system, wherein hydrophobic interactions promoted phase separation and eventually solvent phase partitioning of the system. Therefore, it appears that hydrophilic interactions (e.g., hydrogen bonding) appear to dominate at low dihydric alcohol concentration irrespective of dihydric alcohol structure, while at higher concentration the impact of hydrophobic interactions increase, particularly in the longer diols (1,6-hexanediol and 1,4-butanediol).

Intermolecular interactions (physical entanglement and hydrogen bonding) are important parameters for viscosity enhancement in CA/DMA solutions.[1,4,5] The addition of a hydrogen bond donating nonsolvent can lead to the formation of new hydrogen bonds between the nonsolvent and DMA as well as the nonsolvent and CA, and potentially compete against those between CA and DMA. When FTIR spectroscopy was used, distinct differences in the hydrogen bonding patterns were observed between the various nonsolvents. Figure 2 shows the FTIR spectra of the hydroxyl stretching region of the CA/DMA/nonsolvent systems at 26.6 wt % (clear solutions) and 40.0 wt % (gels) nonsolvent contents. The FTIR spectra of the CA/DMA/dihydric alcohol systems show a dramatic difference between the three nonsolvents. At low nonsolvent contents (26.6 wt %) increasing the alkyl chain length of the dihydric alcohol led not only to less hydrogen bonding but also to the formation of weaker intermolecular hydrogen bonds between components. The FTIR hydroxyl stretching band of the CA/DMA/1,2-ethanediol ternary system (clear solution) indicates a more complex hydrogen bonding system (increased size of the band envelope) with stronger hydrogen bonds (hydroxyl stretching band shifts to lower wavenumber) as compared with that involving 1,4-butanediol, which is more than that involving 1,6-hexanediol. In the absence of CA, the hydroxyl stretching band envelope of the DMA/nonsolvents did not appear any different (data not shown) and was the same as the CA/DMA/1,6-hexanediol at 26.6 wt %. When the dihydric alcohol content was increased to 40.0 wt % a slight shift in the hydroxyl stretching band envelopes was observed. The greatest change was seen for the 1,6-hexanediol system, which expanded to lower wavenumber, becoming identical to that of the 1,4-butanediol system, which like the 1,2-ethanediol system did not significantly change with increasing nonsolvent content. These results further support the involvement of hydrogen bonding[4] but confirm the important role nonbonding interactions play in the development of microstructure and viscoelastic properties.

The rapid increase in viscosity and loss of Newtonian plateau at a low shear rate with increasing nonsolvent concentration suggests the development of a microstructure within the sample and the intensification of intermolecular interactions.[6,7] For all of the dihydric alcohols, a transition from a clear uniform solution to a cloudy system and ultimately a self-supporting gel network was observed with increasing nonsolvent. Figure 3a shows the elastic (G') and viscous (G'') moduli for the CA/DMA/1,4-butanediol ternary system (similar results were obtained for 1,2-ethanediol and 1,6-hexanediol and are shown in Figure S2 of the Supporting Information). At low nonsolvent content (26.6 wt %), G'' is larger than G', and the samples are transparent solutions. Both G' and G'' exhibit strong frequency dependence, reminiscent of a polymer solution. Increasing the 1,4-butanediol content leads to a sol−gel transition at around 36.6 wt %, with $G' \approx G''$ and the system appears cloudy. Further increasing the 1,4-butanediol content to 43.3 wt % increases G' and G'' by several orders of magnitude and the formation of an opaque self-supporting material,[8−10] G' is larger than G'' and is relatively frequency independent, characteristic of a three-dimensional elastic gel.[11−13]

Figure 3b illustrates the effect of increasing dihydric alcohol content on the elastic (G') modulus for each nonsolvent (data obtained at 1 rad s^{-1} from frequency sweep spectra). The elastic modulus, G', increases by over 4 orders of magnitude as the nonsolvent content increases from 0 to ∼35−40 wt %. As previously observed,[1,4,5] a sigmoidal shape with three distinct phases is seen in terms of G' enhancement with increasing nonsolvent content. The elastic modulus initially increases slowly with increasing nonsolvent content (homogeneous solution); then, an intermediate phase of sharp increase in G' and gel formation occurs, followed once again by a slow increase in G'. Although all of the ternary systems exhibit the same sigmoidal shape, the phase of sharp increase in G' happened faster or at a lower nonsolvent content with increasing alkyl chain length of the nonsolvent, albeit the 1,4-butanediol and 1,6-hexanediol exhibiting similar behavior up to gelation, where the 1,6-hexanediol possess significantly larger elastic modulus at the same nonsolvent content.

CLSM analysis of the gels formed using the various dihydric alcohol nonsolvent systems at the same G' (∼60 kPa) and CA concentration (10 and 15 wt %) are shown in Figure 4. The dark blue (top) images represent fluorescent mode images of the samples stained with calcofluor white (a cellulose selective dye). In the fluorescent images, the CA microstructure is shown by the bright-color segments. By contrast, in the reflection images (bottom images, seen in red) the dark areas correspond to the CA domains.[14−17] Here the differences in refractive indices between the CA domains and the solvent/nonsolvent are responsible for image contrast. Clearly the two modes complement each other showing almost identical microstructures, although the images obtained in reflective mode appear to have more microstructural detail. This may be a result of the fact that this technique does not rely on an exogenous fluorescent agent to generate contrast.

There is a clear difference in microstructure between the various gel networks. Increasing the alkyl chain length of the dihydric alcohol nonsolvent appears to lead to a more uniform gel microstructure; a denser network with a more fine and uniform structure is observed as the nonsolvent is changed from 1,2-ethanediol to 1,4-butanediol to 1,6-hexanediol. At 10 wt % CA content (Figure 4a), the change in uniformity appears to

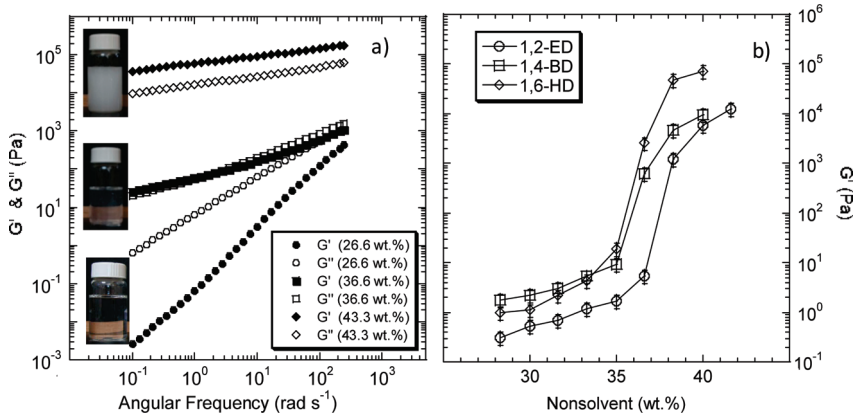

Figure 3. (a) Elastic (G') and viscous (G'') moduli for 15 wt % CA solutions of 1,4-butanediol; clear solution (26.6 wt %), cloudy system (36.6 wt %), and self-supporting gel (43.3 wt.%); (b) Effect of nonsolvent content on elastic modulus (G') for 1,2-ethanediol (1,2-ED), 1,4-butanediol (1,4-BD), and 1,6-hexanediol (1,6-HD) at 15 wt % CA.

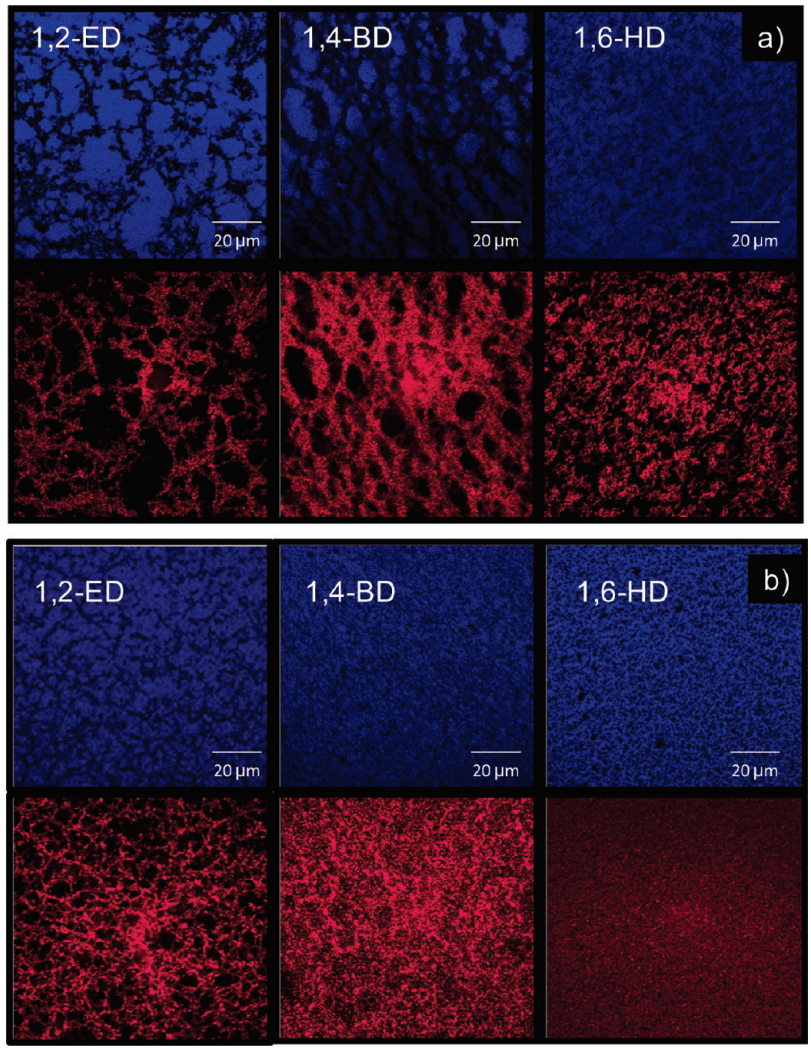

Figure 4. CLSM images of gels at (a) 10 wt % CA concentration and (b) 15 wt % CA concentration at the same elastic modulus ($G' \sim 60$ kPa) for 1,2-ethanediol (1,2-ED), 1,4-butanediol (1,4-BD), and 1,6-hexanediol (1,6-HD) systems. The top CLSM images are fluorescent mode images and the bottom are reflective mode images.

transition well between the three systems, similar to the viscosity behavior observed in Figure 1a. Likewise, at 15 wt % CA the microstructure of 1,2-ethanediol still appears quite different from that of 1,4-butanediol and 1,6-hexanediol, which appear quite similar; again consistent with the viscosity results shown in Figure 1b. However, these results are contrary to those observed for the CA/DMA/monohydric alcohol gels,[4] where increasing the alkyl chain length lead to very inhomogeneous macroporous network structures.

In phase separation induced gelation, morphology is controlled by the interplay between the kinetics of phase separation and the kinetics of gelation.[18,19] For the CA/DMA/monohydric alcohol gels,[4] the extent of hydrogen bonding was low and the kinetics of phase separation was initially faster than gelation.

Table 1. Hansen Solubility Parameters for the Components of the CA/DMA/Dihydric Alcohol Ternary System (δ_d, Dispersive; δ_p, Permanent Dipole−Dipole; δ_h, Hydrogen Bonding; 1,2-Ethanediol (1,2-ED); 1,4-Butanediol (1,4-BD); and 1,6-Hexanediol (1,6-HD))

	solubility parameters $(MPa^{1/2})$[21]			
	δ	δ_d	δ_p	δ_h
CA	25.1	18.6	12.7	11
DMA	22.7	16.8	11.5	10.2
1,2-ED	34.2	17.2	12.6	26.7
1,4-BD	28.3	16.9	7.9	21.2
1,6-HD	25.1	16.5	5.7	18

Increasing the nonsolvent content initiated bulk-phase separation, but as the concentration of components in the CA-rich phase changed, so did the kinetics of phase separation and gelation. The phase-separated morphology for the monohydric alcohol gels appeared as an array of droplets likely obtained via nucleation and growth and spinoidal decomposition of off-critical mixtures. In these systems, the samples quench from the mixed region into the metastable region and incipient droplets redissolve and grow in size. As the extent of hydrogen bonding was low in these systems, the kinetics of phase separation was initially faster than gelation, and as the nonsolvent content increased the system initiated bulk-phase separation. However, as the concentration of components in the CA-rich phase changed, so did the kinetics of phase separation and gelation. In the monohydric alcohol system, as phase separation proceeds, the microstructure coarsens via droplet coalescence and Ostwald ripening, and ultimately gel formation occurred. Based on the 10 wt % CA concentration CLSM images (Figure 4a), the same phenomenon appears to be true for the 1,2-ethanediol system and to a lesser extent the 1,4-butanediol system. However, the 1,6-hexanediol phase-separated gel morphology appears bicontinuous and spinoidal, consistent with that obtained via spinoidal decomposition of near-critical mixtures.[19,20] In this system, as the sample is cooled and spontaneous phase separation occurs, that is, a quench from the mixed region into the unstable region, gelation of the CA retards coarsening and traps the respective microstructure. Increasing the CA content to 15 wt % (Figure 4b), further changes the observed CSLM images and gel morphologies; all of the systems appear to be more bicontinuous and spinoidal as compared to those at 10 wt %. Again, the 1,2-ethanediol system gels appear to undergo more coarsening than the corresponding 1,4-butanediol and 1,6-hexanediol gel systems. In fact, the 1,4-butanediol and 1,6-hexanediol gel systems appear quite similar and quite distinct from that of the 1,2-ethanediol system gels.

A possible explanation for the observed behavior may be due to the different interaction parameters between the different dihydric alcohols, CA and DMA. Polymer−solvent interactions can be estimated based on Hansen solubility parameters and these values are summarized in Table 1. Depending on the nature of the interactions, during phase separation, the dihydric alcohols can segregate to the newly formed interfaces between polymer rich and polymer poor phase separated regions. At these interfaces they (i) reduce the interfacial tension between the phases and reduce the driving force for phase-separation or (ii) form sites for the nucleation and growth of the phase-separated structure. For 1,2-ethanediol, and to a lesser extent 1,4-butanediol systems, the strong nonfavorable interactions with CA are likely driving the phase-separation, and during cooling of the ternary solution, these dihydric alcohols are forming sites for the nucleation and growth of the phase-separated structure. In the case of CA/DMA/1,6-hexanediol system, more favorable interactions exist, and as the spinodal interface matures, the local concentration of 1,6-hexanediol is obviously high enough to induce ordering, resulting in the presentation of a microphase separated structure. The exact mechanism responsible for the structure formation is difficult to isolate from these experiments, and further experiments utilizing scattering and similar techniques will be required to elucidate the dominant kinetic events in this process.

Further information regarding the mechanism of gelation can be obtained by examining the relationship between G' and volume fraction or content of the polymer or, in our case, nonsolvent. If G' exhibits a power-law behavior with nonsolvent content (Φ), that is, $G' \approx \Phi^n$, the gels may be fractal in nature. All of the dihydric alcohol nonsolvent systems exhibit power-law behavior between G' and nonsolvent content (Figure 5). The power-law exponents varied between the various systems. At 10 wt % CA content (Figure 5a) the power-law exponents increased from 23 for 1,2-ethanediol and 1,4-butanediol to 60 for 1,6-hexanediol, whereas at 15 wt % CA (Figure 5b) 1,2-ethanediol system remains unchanged at 23, but both 1,4-butanediol and 1,6-hexanediol systems increased slightly to 30 and 75, respectively. The similar power-law exponent values of the 1,2-ethanediol and 1,4-butanediol system gels at 10 wt % CA content, and the similarity in morphology (Figure 4a) suggests that their gelation mechanism is similar[22] and different than that of the 1,6-hexanediol system (as discussed above). However, at 15 wt % CA content, the 1,2-ethanediol system power-law exponent value does not change, while that of 1,4-butanediol and 1,6-hexanediol systems increase by the same amount ~25−30%. This, combined with the similar CSLM

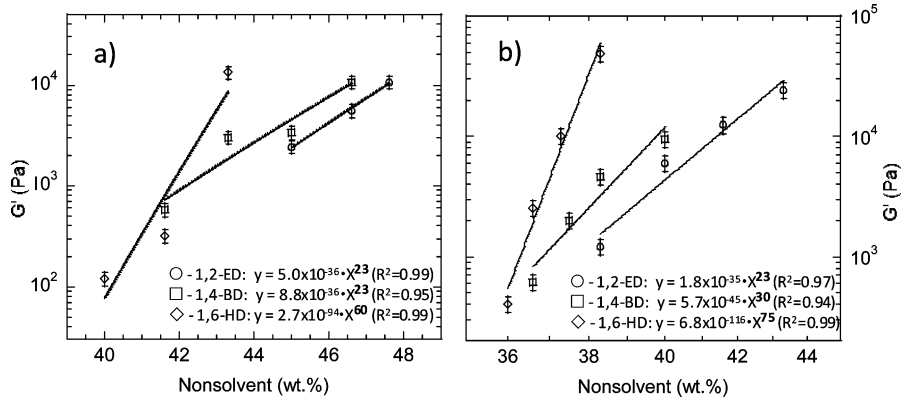

Figure 5. Elastic modulus (G' obtained at frequency of 1 rad s^{-1}) of CA/DMA/dihydric alcohol gels as a function of nonsolvent content at (a) 10 wt % CA and (b) 15 wt % CA content: 1,2-ethanediol (1,2-ED); 1,4-butanediol (1,4-BD); 1,6-hexanediol (1,6-HD).

morphologies (Figure 4b), may indicate that at the more concentrated CA conditions the gelation mechanism of the 1,4-butanediol system is more like that of the 1,6-hexanediol system.

Fractal gels can be classified as either strong-linked or weak-linked systems. In strong linked systems, the links between flocs are stronger than those within the flocs, and as a result, failure under deformation occurs through breaking intrafloc interactions. As such, this leads to a decrease in the LVE regime with increasing sample concentration. By contrast, weak-linked gels possess strong intrafloc links, more rigid than the interfloc linkages, and an increase in the limit of linearity occurs with increasing concentration. In all of the dihydric alcohol systems the onset of nonlinearity shifted to lower value with increasing concentration (Figure S3 of the Supporting Information), indicating the CA/DMA/dihydric alcohol gels are strong-linked.

As the gels are strong-linked aggregated macromolecules, their fractal dimensions can be determined through confocal microscopy[1,4,5,22−24] by the box counting technique using Image J software.[23] In this method, the scaling relation is $N \propto r^{-D}$, where N is the number of boxes filled with CA, r is the size of the square box, and D is the fractal dimension of the CA network. From the CLSM images (Figure 4), the fractal dimension of the gels was determined and found to vary slightly between the three systems. The 1,2-ethanediol and 1,4-butanediol systems have fractal dimensions of $D \sim 1.87 \pm 0.02$, slightly lower than that of 1,6-hexanediol at $D \sim 1.97 \pm 0.02$ and suggest potentially different mechanisms: faster cluster−cluster aggregation (CLCLA) for 1,2-ethanediol and 1,4-butanediol systems and a slower reaction-limited aggregation (RLA) mechanism for 1,6-hexanediol system.[22] However, at 15 wt % CA content, the fractal dimension of the three systems is the same, $D \sim 1.97 \pm 0.03$, despite the visually apparent differences between the three gel networks morphology. This again may point to the limitation in sensitivity of the fractal dimension.[4,25]

Conclusions

The effect of nonsolvent structure on the phase behavior and viscoelastic properties of a CA/DMA/nonsolvent ternary system was investigated using steady state and dynamic rheology. At low nonsolvent concentration, Newtonian behavior was observed, followed by shear thinning at high shear rates. Increasing nonsolvent concentration enhanced the intermolecular interactions, and the system exhibited non-Newtonian behavior at a low shear rate, representing the development of microstructure. Changing the properties of the dihydric alcohol nonsolvent by increasing the alkyl chain length enhanced solution viscosity and modulus, the extent of which being dependent on CA concentration. At high nonsolvent concentrations, phase separation and gelation occurred, the mechanism of which was dependent on the nonsolvent. In the case of 1,2-ethanediol and 1,4-butanediol systems, the phase-separated gel morphologies at 10 wt % CA content were consistent with that obtained via nucleation and growth and spinoidal decomposition, while that of 1,6-hexanediol gels likely arising via spinoidal decomposition. Increasing CA content to 15 wt % increased the uniformity of the gels. In particular, the 1,4-butanediol system morphologies appear comparable to that of the 1,6-hexanediol system. In the case of the 1,2-ethanediol and 1,4-butanediol systems, increasing CA content likely changes the kinetics of phase separation and gelation, particularly in the 1,4-butanediol system wherein the extent of coarsening is substantially decreased. Rheological and microscopic analyses further revealed the various gels are fractal in nature, and can be classified as strong-linked gel networks. At low CA content (10 wt %), the various gel networks exhibited different fractal dimensions in-line with the observed differences in microstructure: $D \sim 1.87 \pm 0.02$ (1,2-ethanediol and 1,4-butanediol) and $D \sim 1.97 \pm 0.02$ (1,6-hexanediol). However, at 15 wt % CA content, the gels exhibited more similar viscoelastic behavior and gel microstructures; $D \sim 1.97 \pm 0.02$ for all three dihydric alcohol systems.

Acknowledgment. The authors greatly acknowledge the Natural Sciences and Engineering Research Council of Canada (STPGP 336241) for financial support of this research.

Supporting Information Available. Steady state and dynamic rheology data. This material is available free of charge via the Internet at http://pubs.acs.org.

References and Notes

(1) Appaw, C.; Gilbert, R. D.; Khan, S. A.; Kadla, J. F. Viscoelastic Behavior of Cellulose Acetate in a Mixed Solvent System. *Biomacromolecules* **2007**, *8* (5), 1541–1547.
(2) Hong, P.-D.; Chou, C.-M.; Huang, H.-T. Phase separation behavior in polyvinyl alcohol/ethylene glycol/water ternary solutions. *Eur. Polym. J.* **2000**, *36*, 2193–2200.
(3) Hong, S.-J.; Hong, P.-D.; Chen, J.-C.; Shih, K.-S. Effect of Mixed Solvent on Solution Properties and Gelation Behavior of Poly(vinyl alcohol). *Eur. Polym. J.* **2009**, *45*, 1158–1168.
(4) Kadla, J. F.; Korehei, R. Effect of Hydrophilic and Hydrophobic Interactions on the Rheological Behavior and Microstructure of a Ternary Cellulose Acetate System. *Biomacromolecules* **2010**, *11* (4), 1074–1081.
(5) Appaw, C.; Gilbert, R. D.; Khan, S. A.; Kadla, J. F. Phase Separation and Heat-Induced Gelation Characteristics of Cellulose Acetate in a Mixed Solvent System. *Cellulose* **2010**, *17* (3), 533–538.
(6) Fang, Y. P.; Takahashi, R.; Nishinari, K. Rheological Characterization of Schizophyllan Aqueous Solutions after Denaturation-Renaturation Treatment. *Biopolymers* **2004**, *74* (4), 302–315.
(7) Steiner, W.; Lafferty, R. M.; Gomes, I.; Esterbauer, H. Studies on a Wild Strain of Schizophyllum-Commune: Cellulase and Xylanase Production and Formation of the Extracellular Polysaccharide Schizophyllan. *Biotechnol. Bioeng.* **1987**, *30* (2), 169–178.
(8) Nielsen, L. E. *Polymer Rheology*; Marcel Dekker: New York, 1977; p 203.
(9) Ferry, J. D. *Viscoelastic Properties of Polymers*, 3rd ed.; Wiley: New York; Toronto, 1980; p 641.
(10) Macosko, C. W. *Rheology: Principles, Measurements, and Applications*; VCH: New York, NY, 1994; p 550.
(11) Cai, J.; Zhang, L. Unique Gelation Behavior of Cellulose in NaOH/Urea Aqueous Solution. *Biomacromolecules* **2006**, *7* (1), 183–189.
(12) Winter, H. H.; Mours, M. Rheology of Polymers near Liquid-Solid Transitions. *Neutron Spin Echo Spectrosc. Viscoelasticity Rheol.* **1997**, *134*, 165–234.
(13) da Silva, M. A.; Areas, E. P. G. Solvent-Induced Lysozyme Gels: Rheology, Fractal Analysis, and Sol-Gel Kinetics. *J. Colloid Interface Sci.* **2005**, *289* (2), 394–401.
(14) Ljunglof, A.; Bergvall, P.; Bhikhabhai, R.; Hjorth, R. Direct Visualisation of Plasmid DNA in Individual Chromatography Adsorbent Particles by Confocal Scanning Laser Microscopy. *J. Chromatogr., A* **1999**, *844* (1−2), 129–135.
(15) Fang, N.; Lai, A. C. K.; Wan, K. T.; Chan, V. Effect of Acyl Chain Mismatch on the Contact Mechanics of Two-Component Phospholipid Vesicle during Main Phase Transition. *Biophys. Chem.* **2003**, *104* (1), 141–153.
(16) Charcosset, C.; Bernengo, J. C. Comparison of Microporous Membrane Morphologies Using Confocal Scanning Laser Microscopy. *J. Membr. Sci.* **2000**, *168* (1−2), 53–62.
(17) Charcosset, C.; Cherfi, A.; Bernengo, J. C. Characterization of Microporous Membrane Morphology Using Confocal Scanning Laser Microscopy. *Chem. Eng. Sci.* **2000**, *55* (22), 5351–5358.
(18) Bansil, R.; Liao, G. D. Kinetics of Spinodal Decomposition in Homopolymer Solutions and Gels. *Trends Polym. Sci.* **1997**, *5* (5), 146–154.
(19) Butler, M. F.; Heppenstall-Butler, M. Phase Separation in Gelatin/Dextran and Gelatin/Maltodextrin Mixtures. *Food Hydrocolloids* **2003**, *17*, 815–830.

(20) Tsunashima, Y.; Kawanishi, H.; Horii, F. M. Reorganization of Dynamic Self-Assemblies of Cellulose Diacetate in Solution: Dynamical Critical-Like Fluctuations in the Lower Critical Solution Temperature System. *Biomacromolecules* **2002**, *3* (6), 1276–1285.
(21) Grulke, E. A. Solubility parameter values. In *Polymer Handbook*; Brandrup, J., Immergut, E. H., Grulke, E. A. Eds.; John Wiley & Sons: NY, 1999; pp 675−714.
(22) Shih, W. H.; Shih, W. Y.; Kim, S. I.; Liu, J.; Aksay, I. A. Scaling Behavior of the Elastic Properties of Colloidal Gels. *Phys. Rev. A* **1990**, *42* (8), 4772–4779.
(23) Eissa, A. S.; Khan, S. A. Acid-Induced Gelation of Enzymatically Modified, Preheated Whey Proteins. *J. Agric. Food Chem.* **2005**, *53* (12), 5010–5017.
(24) Marangoni, A. G. The Nature of Fractality in Fat Crystal Networks. *Trends Food Sci. Technol.* **2002**, *13* (2), 37–47.
(25) Pugnaloni, L. A.; Matia-Merino, L.; Dickinson, E. Microstructure of Acid-Induced Caseinate Gels Containing Sucrose: Quantification from Confocal Microscopy and Image Analysis. *Colloids Surf., B* **2005**, *42* (3−4), 211–217.

BM100917J